

Landslide Stability Analysis and Prediction Modeling with Landslide Occurrences on KOMPSAT EOC Imagery

Kwang-Hoon Chi*, Kiwon Lee**, and No-Wook Park*

National Geoscience Information Center, Korea Institute of Geoscience and Mineral Resources*

Department of Information Systems (GIS/RS), Information and Computer Science Div., Hansung University**

Abstract : Landslide prediction modeling has been regarded as one of the important environmental applications in GIS. While, landslide stability in a certain area as collateral process for prediction modeling can be characterized by DEM-based hydrological features such as flow-direction, flow-accumulation, flow-length, wetness index, and so forth. In this study, Slope-Area plot methodology followed by stability index mapping with these hydrological variables is firstly performed for stability analysis with actual landslide occurrences at Boeun area, Korea, and then landslide prediction modeling based on likelihood ratio model for landslide potential mapping is carried out; in addition, KOMPSAT EOC imagery is used to detect the locations and scarped scale of landslide occurrences. These two tasks are independently processed for preparation of unbiased criteria, and then results of those are qualitatively compared. As results of this case study, land stability analysis based on DEM-based hydrological variables directly reflects terrain characteristics; however, the results in the form of land stability map by landslide prediction model are not fully matched with those of hydrologic landslide analysis due to the heuristic scheme based on location of existed landslide occurrences within prediction approach, especially zones of not-investigated occurrences. Therefore, it is expected that the results on the space-robustness of landslide prediction models in conjunction with DEM-based landslide stability analysis can be effectively utilized to search out unrevealed or hidden landslide occurrences.

Key Words : Hydrological Characteristics, Landslide prediction, Landslide stability, Likelihood Ratio Model, Slope-Area Plot.

1. Introduction

GIS to hydrological applications for landslide prediction modeling, in other name of landslide hazard mapping, has been regarded as one of the important application fields (Wilson *et al.*, 2000). While, hydrological application of GIS to landslide analysis is

somewhat concentrated on the environmental spatial data integration using multiple data sets followed by concerned database building, as well as new algorithm development/evaluation and comparison with previous ones. The hydrological application and concerned algorithm of GIS have been studied in various approaches: hydrological objected-oriented data modeling (Hellweger and Maidment, 1999; Davis,

2000), drainage basin and watershed analysis (O'Loughlin, 1986; Dietrich *et al.*, 1993; Garbrecht and Martz, 1997; Smith *et al.*, 1997; Tarboton, 1997; Mason and Maidment, 2000), and landslide-related hydrological characterization (Montgomery *et al.*, 1994; Wu and Sidle, 1995; Montgomery *et al.*, 1998; Pack *et al.*, 1998). Also, several customizable functions to extract basic hydrological features such as flow direction, flow accumulation, flow length and watershed delineation are provided in most commercialized GIS with full-featured functions.

Meanwhile, digital representation in the multiple geo-based data sets is towards spatial quantitative modeling that combines the distribution of spatial features in each mappable data set or layer into a target-oriented theme. This rationale or scheme, dealing with geoscientific data integration in mineral potential mapping (Moon, 1990; An *et al.*, 1991; Chung and Fabbri, 1993), can also be applied in spatial prediction models in landslide hazard mapping. It is known that these approaches with their own mathematical backgrounds have provided powerful schemes for decision-supporting information, through

several case studies for landslide hazard mapping (Van Westen, 1993; Chung and Fabbri, 1999).

In landslide hazard mapping, "When, Where and What scale" of landslides are important aspect in prediction. All predictions related to future events are always subject to the uncertainties. For the planning of future land use, an essential component is the identification of areas that are affected by future landslide. So the prediction models not only identify vulnerable areas but also estimate the uncertainties associated with the predictions. However, proper interpretation and quantitative evaluation of prediction result have not been fully considered in landslide hazard mapping. Recently emphasis has been directed towards the application strategies that include the validation and stability analysis of the model (Chung *et al.*, 2001; Fabbri and Chung, 2001).

Meanwhile, the hydrologic characteristics, such as wetness index and saturation index, extracted from DEM (Digital Elevation Model) can be utilized in actual landslide analysis and hazard mapping mentioned above, if landslide occurrences are taken

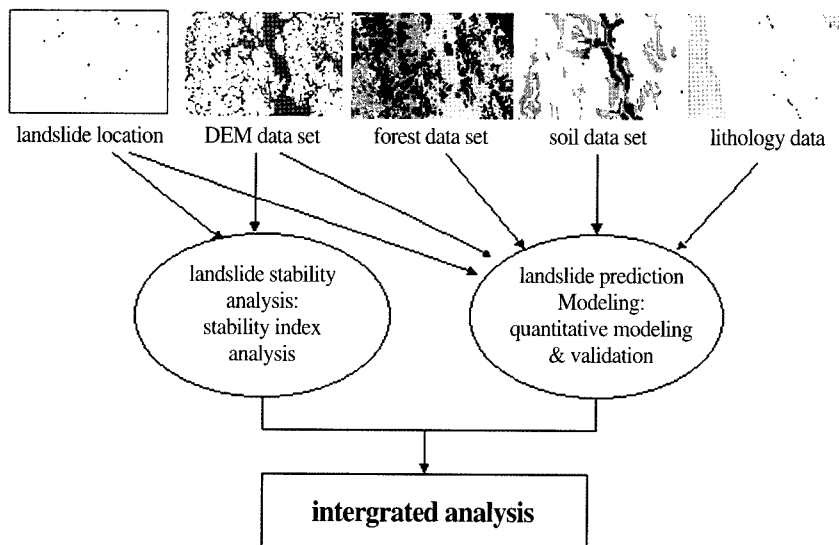


Fig. 1. Schemes applied for landslide stability analysis and prediction modeling.

into account, because hydrological variables are regarded as one of the most influenced factors in landslide prediction model. However, there are a few case studies or published works on landslide modeling with landslide analysis based on actual landslide occurrences or detectable landslide features in satellite imagery.

In this study, the landslide analysis with hydrological variables and the landslide prediction modeling are performed using ArcInfo and ArcView with hydrological application programs under Spatial Analyst, proposed and implemented by Tarboton (1997) and Pack *et al.* (1998). Furthermore, for testing on the space-robustness of landslide prediction models, we exemplify whether and to what extent a prediction can be extended, in space, to neighboring areas with similar geomorphology or geology using the validation and stability analysis of the model, using spatial data sets from Boeun, Korea (Fig. 1).

2. Study Area and Data Sets

The Boeun area, Korea, which had suffered from lots of landslide damages due to the heavy rain in summer, 1998, is selected for the case study area. The input data (termed “causal factor”) for landslide prediction modeling consists of several layers of map information (Table 1). The slope and aspect are directly calculated from the DEM, using common functions. As for the soil data sets, the texture, topography, drainage, material, and thickness of soil are acquired from a paper soil map. As for the forest data sets, the forest type and diameter, age, and density of timber are digitized from forest maps produced by Korea Forest Research Institute. While, the lithological map is obtained from a geological map of KIGAM. These data sets are built on a cell-based database in GIS environment, and the whole study area consists of $1,270 \times 722$ pixels, covering approximately

Table 1. Description of the data sets used in the study area.

Type	Data set
Landslide location	30 locations
Topography	Digital Elevation Model Slope Aspect
Forest*	Forest Type Timber Diameter Timber Age Forest Density
Soil**	Texture Drainage Soil Type Thickness
Geology***	Lithology

* Forest map of Boeun, Kwanki, 1:25,000, Korea forest service, Korea forest research institute.

** Detailed interpretative soil maps of Boeun -gun, 1:25,000, Rural development administration, Agricultural sciences institute, 1993.

*** Geological map of Boeun, Chongsan, 1:50,000, Korea institute of geoscience and mineral resources, 1977, 1986.

92km². Each pixel on these data is referenced to a 10m by 10m area on the ground for data integration for landslide hazard mapping.

As for the landslide locations, the aerial photographs taken in 1996 and 1999, and KOMPSAT EOC imagery were firstly used to detect them, and the locations were verified in the field, done in site investigation after landslide events. While, those landslide occurrences were recognized on the KOMPSAT EOC imagery in Fig. 2(a), about 30 landslides. The target pattern, with the entire landslide bodies, consists of two separate and distinct sub-areas: the scarp area and the deposit area. The geomorphologic characteristics of these two sub-areas are distinctly different. Hence, it is necessary to define the scarps of the future landslides as the new target pattern rather than the whole scars of the landslides. In this study, the topographically highest 20% of the scars of the landslides are considered as trigger areas. Though landslide occurrences are small-

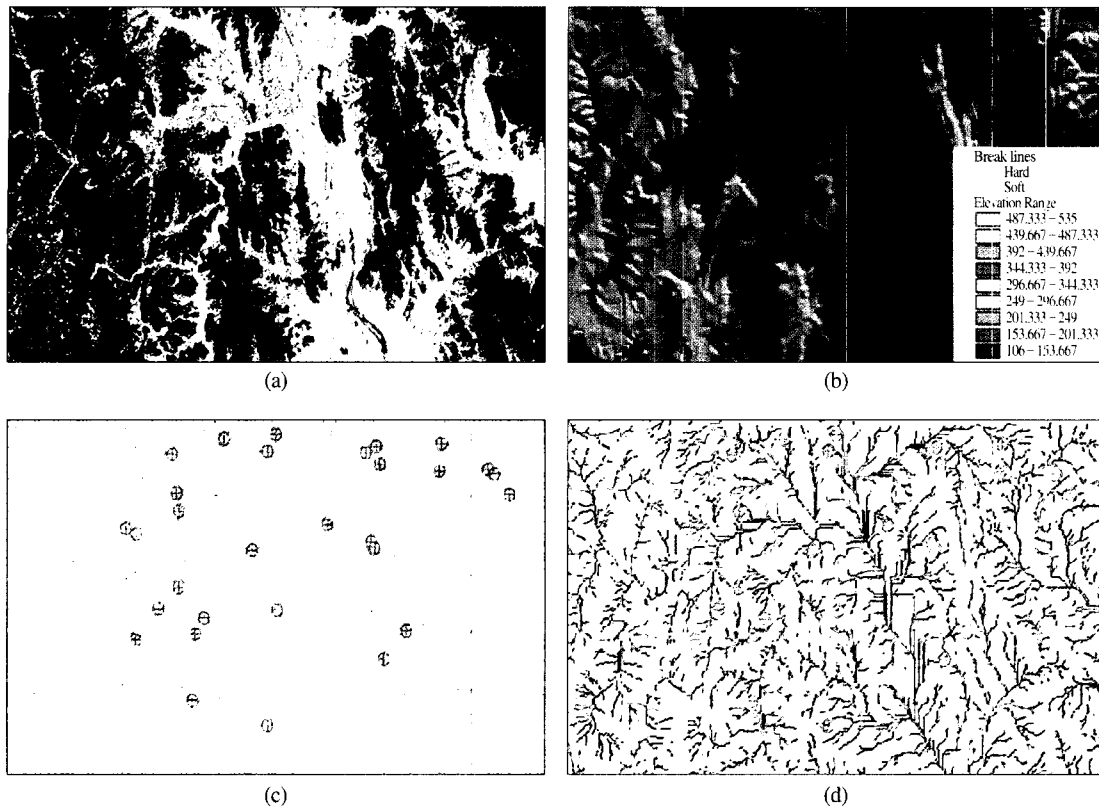


Fig. 2. (a) Landslide occurrences superimposed on the KOMPSAT EOC imagery, (b) Sink-removed DEM-based 3D View of the case study area in meter unit: Boeun region, Korea: Coverage (1270 × 722) with cell unit of 10 meters, in the rectangle region of left top: 127° 38' 53'' E, 36° 29' 58'' N and right bottom: 127° 47' 21'' E, 36° 26' 01'' N, (c) 10m-interval Topographic map of the study area coverage with actual landslide scarped zones as point feature, and (d) Stream network model in the study area with landslide point features.

scaled, tens of occurrences in one or two days were recorded, due to the relative terrain changes in slope and aspect (Fig. 2(b)). Landslide patterns are also revealed at topographic relief (Fig. 2(c)), and these occurrences were converted into point features. However, these occurrences are verified by field observation; therefore, they are not all occurrences, covering unrevealed and unverified. While Fig. 2(d) represents stream network, composed of those areas where concentrated flow is occurring, with actual occurrences, by Strahler stream ordering with 200 m and 100 m intervals. Strahler stream ordering is computed by only increases when streams of the same order intersect, under given interval. It is shown that

this network overlaid landslide occurrences reflects hydrological characteristics due to shallow the transitional land-sliding controlled by shallow groundwater flow convergence.

3. Hydrological Characteristics related to Landslide Stability

As for shallow land-sliding, several hydrological variables extracted from sink-removed DEM (Fig. 2(b)) provide useful information for landslide analysis. Among them, flow direction (Fig. 3(a)) is a variable on how many cells flow into any given cell, and flow

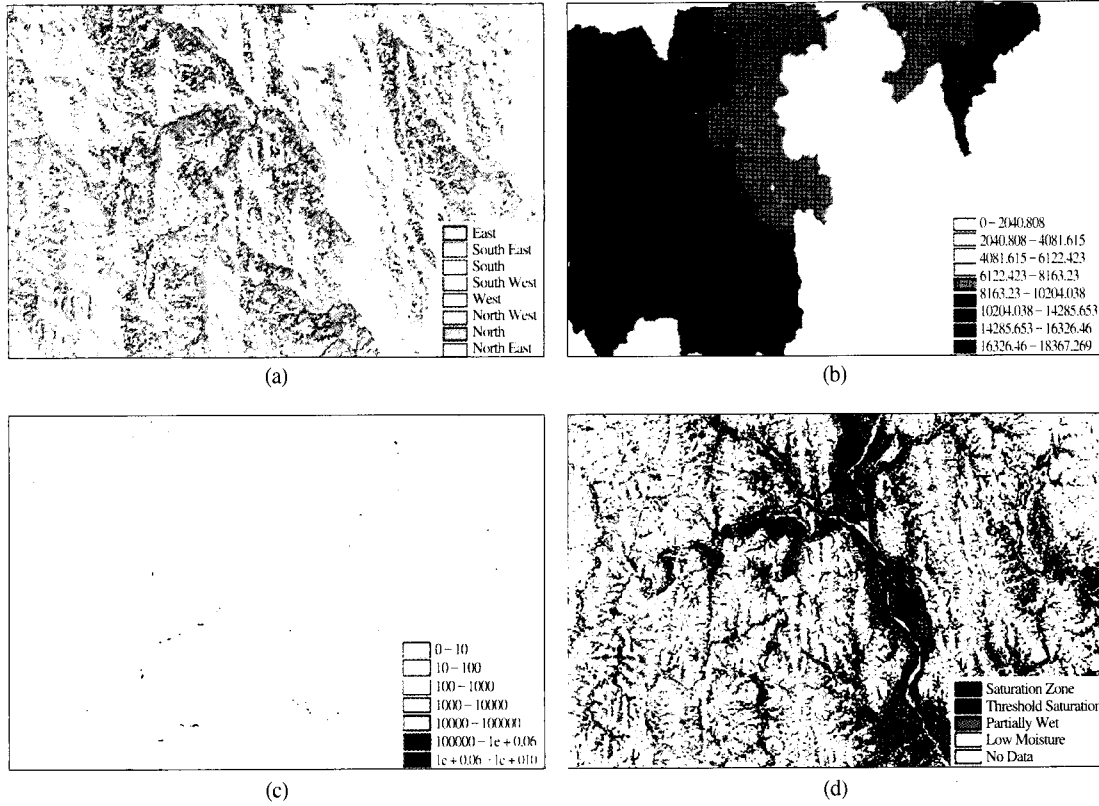


Fig. 3. (a) Flow direction mapping in unit of 8 types of azimuthal direction, (b) Downstream flow length mapping in meter unit, (c) Contributing area mapping, and (d) Saturation index mapping for wetness.

length (Fig. 3(b)) represents what areas have more water flowing through them than others and the length of the longest flow path within a drainage region or basin. As well as these hydrological variables, several indices in associated with landslide stability also can be extracted with respect to contributing area (Fig. 3(c)), computed as a field representing at each point the magnitude of the drainage area upslope of that point. In terms of specific catchment area, it is a field representing contributing area per unit contour width.

Wetness index terms a quantity of contributing catchment area in squared divided by slope of cell in degrees, and can be interpreted in the categorical classes (Fig. 3(d)), as a kind of indicator of erosive sensitivity of overland flow.

4. Stable Index Mapping and S-A Plot for Calibration

With theoretical basis of 'Infinite Plane Slope Stability Model' (Montgomery and Dietrich, 1994), Stability index is defined as $P(\text{Factor of safety} > 1)$ with uncertainty range; according to Pack *et al.* (1998), the term of Factor of safety (FS) can be formulated with variables: topographic slope angle, relative wetness (w), and dimensionless cohesion (C), shown in equation (1).

$$FS = \frac{C + \cos\theta[1-wr]\tan\phi}{\sin\theta} \quad \text{where} \quad (1)$$

$$w = \min\left(\frac{Ra}{T\sin\theta}, 1\right), C = (C_r + C_s)/(h\rho_s g), \text{ and } r = \rho_w/\rho_s.$$

θ : slope angle, ϕ : soil internal friction angle, R : Recharge, a : specific catchment area, T : soil transmissivity, $h\rho_s g$: soil weight, C_r , C_s , ρ_w and ρ_s : root and soil cohesion, water density and soil density, respectively

While, this index as spatial distribution represents shallow subsurface groundwater flow convergence and topographic slope, with uncertainty parameter incorporated through ranges of soil and hydrological parameters, not being applicable to deep-seated instability, and it is a kind of extensible model based on the infinite plane slope stability model with topographically based wetness to account for parameter uncertainty (Pack *et al.*, 1997). Tarboton (1997) proposed and implemented some criteria to classify landslide stability index which maps potential landslide initiation zones with 6 types by SI values: ① Stable or safety ($SI > 1.5$), ② Moderately stable ($1.5 > SI > 1.25$), ③ Quasi-stable ($1.25 > SI > 1.0$), ④ Lower threshold slope ($1.0 > SI > 0.5$), ⑤ Upper threshold slope ($0.5 > SI > 0.0$), and ⑥ Defended slope or instability to need defended ($0.0 > SI$). Based on these classes, summary statistics on landslide occurrence in this area is given at Table 2. The relatively stable classes of ① Stable, ② Moderately stable, and ③ Quasi-stable are approximately 76% of 30 landslide occurrences, counted in landslide analysis.

In this study, all landslide occurrences are not investigated in the field survey. Moreover, the classification of landslide types by cause effect or hazardous zone is not considered in this study. While, the centered location of most scarped areas in the field survey is categorized into landslide point feature. Therefore, it is not enough that lower percentage of landslide occurrences at potential instability zones of

④ Lower threshold slope, ⑤ Upper threshold slope, and ⑥ Defended slope represent real situation of landslide characteristics in this area, according that landslide density of lower/Upper threshold slope class is rather higher than one of other classes (Fig. 4(a)).

S(Slope)-A(Area) plot for landslide stability index, proposed by Pack *et al.*(1997), is applied in this study (Fig. 4(b)). S-A plot is interpreted as a kind of calibration plot with several calibration region parameters of LTR, UTR, LC, UC, LFA, and UFA which stands for Lower and Upper bound of R/T, Lower and Upper bound of Dimensionless Cohesion, Lower and Upper bound of soil friction angle (ϕ); in this study, these parameters were used as 2000, 3000, 0., 0.25, 30° and 40°, respectively. These bounds define uniform probability distributions over which these quantities are assumed to vary at random, and this uniform distributions which lower and upper bounds as

$$\begin{aligned} C &\sim U(C_L, C_U) \\ R/T &\sim U(R_L/T_U, R_U/T_L) \\ \tan \phi &\sim U(\tan \phi_L, \tan \phi_U) \end{aligned} \quad (2)$$

While, these parameters are not based on the field measures in this study area, but experiment parameters by Pack *et al.*(1998) in consideration to uncertainty bounding. Therefore, it is expected that exact field measures in this area would be within these bounds. While, saturation level such as saturated, unsaturated, and wetness 10 % is also represented by using equation (1), in the term of w . Therefore, this SA plot can be used

Table 2. Statistics of landslide occurrences in the study area.

	Stable	Moderately Stable	Quasi-Stable	Lower Threshold Slope	Upper Threshold Slope	Defended Slope	Total
% Region	64.8	3.4	19.8	8.1	3.6	0.3	100
Number of Landslide	14	1	8	5	2	0	30
% Landslide	46.7	3.3	26.6	16.7	6.7	0.0	100
Landslide Density	0.2	0.3	0.5	0.7	0.6	0.0	0.3

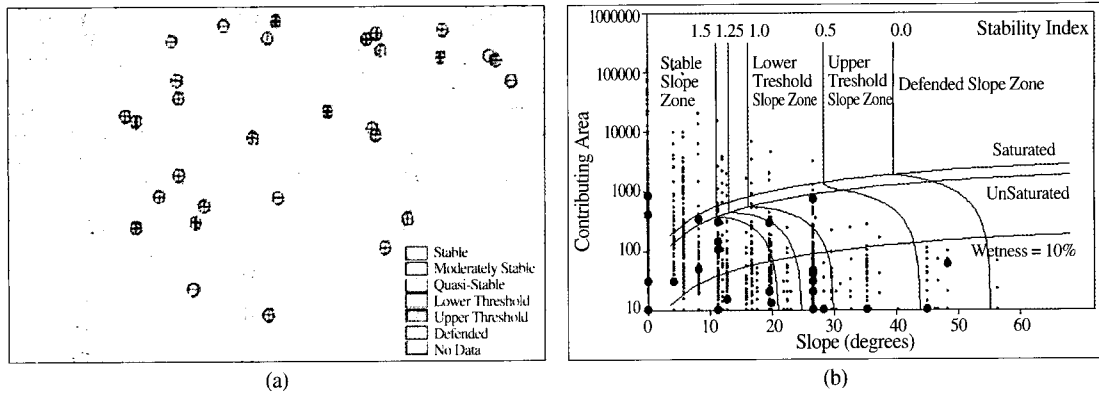


Fig. 4. (a) Landslide stability index mapping at Boeun area in 6 classes (b) An example of S-A plot at Boeun area, Korea, in consideration of actual landslide occurrences (solid circle on plot); LTR(2000m), UTR(3000m), LC(0.0), UC(0.25), LFA(30°), and UFA(40°).

to elucidate hydrological characteristics related to actual landslide occurrences, in the slope-area space.

5. Landslide Prediction Model

Among many prediction models for landslides, in this study, we have implemented a landslide prediction model based on the likelihood ratio model proposed by Chung and Fabbri (1998). The likelihood ratio model employed in this study is described briefly here.

To identify the hazard areas for potential or unrevealed landslides, we want to separate two sub-

areas, the hazardous sub-areas affected by landslides and the non-hazardous sub-areas not affected by landslides. Suppose that the study area is divided into two non-overlapping sub-areas, above two sub-areas. If fundamental variables such as slope, aspect, and so on are provided, then the data from the hazardous sub-areas should have unique characteristics that are different from the data from the non-hazardous sub-areas. This suggests that the probability frequency distribution functions of the hazardous and the non-hazardous sub-areas should be distinctly different. The likelihood ratio function, which means the ratio of the two frequency distribution functions, can highlight this difference.



Fig. 5. Prediction map of landslide hazard in Boeun area using the likelihood ratio function.

Consider the study area **A**, and a pixel **p** in **A** and a proposition:

$$T_p : \text{"p will be affected by the future landslide of type D"} \quad (3)$$

For each *k*-th layer L_k , the *m* layers of map data at every **p** in **A** are represented, in a quantized form by:

$$\{c_k(p), k = 1, \dots, m, \mathbf{A}\} \quad (4)$$

where, $c_k(p)$ is the quantized value for the *k*-th layer L_k at **p**.

Then, in probability framework, measurement of the "sureness" that the proposition T_p is true, given the *m* causal factors ($c_k(p), k = 1, \dots, m$) at **p** is assumed to be the joint conditional probability function.

$$\text{Favorability function} \{T_p | c_k(p)\} = \text{Prob}\{T_p | c_k(p)\} \quad (5)$$

Above function value indicates that how each of the *m* pieces of evidence ($c_k(p), k = 1, \dots, m$) supports the "sureness" that the proposition is true at **p**. Suppose M_p denotes the proposition that **p** comes from the area affected by landslides, and \bar{M}_p from **p** comes from the area not affected by landslides. Also, let $\text{Prob}(c_k(p) | M_p)$ and $\text{Prob}(c_k(p) | \bar{M}_p)$ be the empirical frequency distribution function of area affected by landslides and that of area not affected by landslides, respectively.

Then likelihood ration function λ_p can be calculated as follows:

$$\begin{aligned} \lambda_p(c_k(p)) &= \text{Prob}\{c_k(p) | M_p\} / \text{Prob}\{c_k(p) | \bar{M}_p\} \\ &= \frac{1 - \text{Prob}\{M_p\}}{\text{Prob}\{M_p\}} \cdot \frac{\text{Prob}\{M_p | c_k\}}{1 - \text{Prob}\{M_p | c_k\}} \quad (6) \end{aligned}$$

For each data layer, two empirical distribution functions for the hazardous sub-areas and the non-hazardous sub-areas are computed by using the Bayesian combination rule, and then the likelihood ratio functions for all data layers are combined. The prediction maps can be obtained from these joint likelihood ratio functions.

To visualize a prediction map, we used rank order statistics. We first computed the score for each pixel and

then sort all scores by increasing order to determine the ranks of the scores. The pixel that has the smallest score (the smallest prediction value) has rank one, and the pixel that has the maximum score has the maximum rank, 916940, the total number of pixels. Then the ranks are normalized so that the maximum value is 1 or 100% and the normalized values are termed the favourability indices or simply indices. The pixel with the index 100% had the largest score of the prediction function. If the pixels have index, 99.5%, it means that the ranks of their function scores are within the top 0.5% (99.5% – 100%) in the study area. These indices over the study area constitute a prediction map. In Fig. 5, we delineate the areas that show high landslide hazard, and overall, the resultant layer fitted the real situation, showing in the past landslides.

The next question in prediction modeling is how successful this prediction map would be with respect to the future landslides. It leads to the next essential step of validation.

6. Analytical Procedure for Space-Robustness

The critical strategy in prediction models is the task of validating the prediction results, so that the prediction results can provide meaningful interpretation with respect to the future landslides. To carry out the validation, we must restrict the use of all the data of the past landslides in the study area. By partitioning the data, one subset is used for obtaining a prediction map; the other subset is compared with the prediction results for validation. To establish whether and to what extent a prediction can be extended, in space, to neighboring areas with similar geology, we divided the entire study area into two separated sub-areas. We selected one of two sub-areas to construct a prediction model and the other to validate the prediction. When we use this space-

partition technique, then we are able to extend the current prediction model in the study area to the surrounding areas or similar geology. It represents a form of data mining where the study area and the respective database are subdivided into two parts so that the spatial data from one part is used to compute the prediction over the entire area, and the landslides distribution from another part is used to validate it. Then the predicted parts that can be validated can be assembled into a mosaic of predictions.

The study area has been subdivided into a northern sub-area and a southern sub-area. This was because the

geological trend runs in the north-south direction so that greater similarity exists between north-south than east-west sub-areas, and the corresponding database subdivisions.

This space-partition technique has been used as follows (Fig. 6): (i) the 21 scarps distributed in the north sub-area together with the corresponding spatial database were used to compute the south sub-area prediction model, and (ii) similarly the 9 scarps in the south sub-area with the corresponding spatial database were used to compute the north sub-area prediction model. Then we assembled them into a mosaic of the

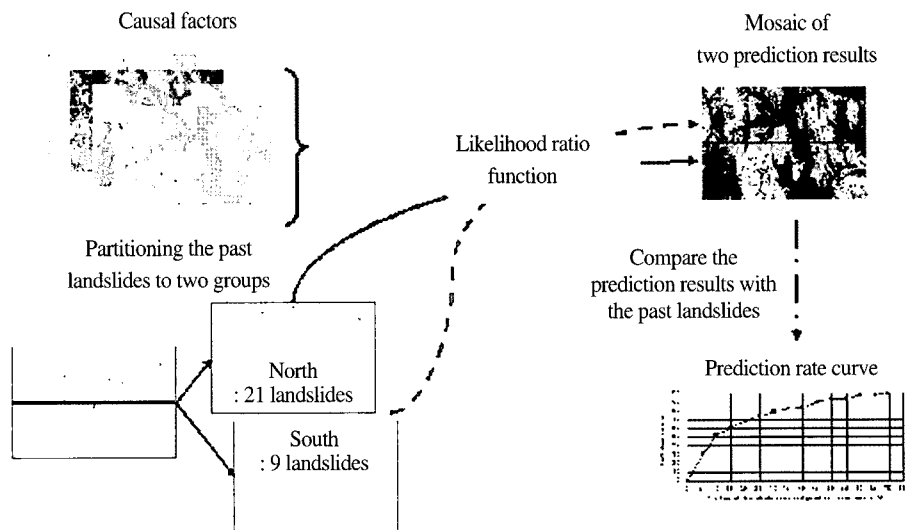


Fig. 6. Procedure for testing on the space-robustness of landslide prediction model.

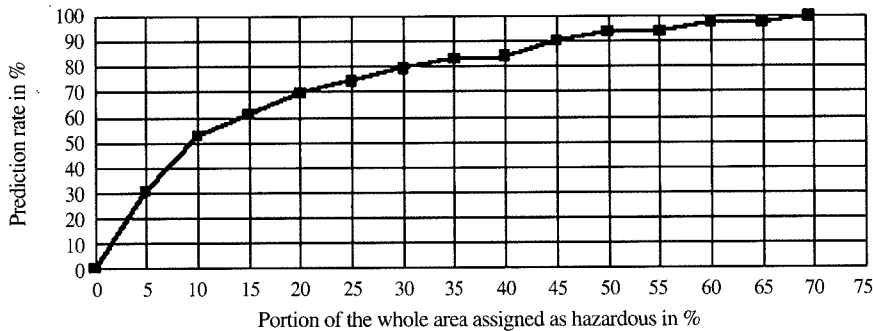


Fig. 7. Prediction rate curve for a mosaic of two predictions.

two representations. To validate a mosaic prediction map, we computed the prediction rate curve, which can explain the proportion of pixels correctly classified for the whole scarps in a mosaic map (Fig. 7). This prediction rate curve relates to the number of the future landslides and to the probability of the occurrences of the future landslides (Chi *et al.*, 2001).

To interpret the curve for a prediction image in Fig. 5, consider a point (10, 52.5) on the curve in Fig. 7(b). For the future landslides, if we take the most hazardous 10% area of the corresponding prediction image in Fig. 5, then we may estimate that 52.5% of all future landslides will be located in the delineated area. Therefore, if we wish to delineate areas, which should identify at least 52.5% of the future landslides, then we can declare 10% of the study area a hazardous area.

For any prediction models to generate reasonably “good or significant” results, the prediction result should be robust and stable (Chung *et al.*, 2001). Through above space-partition technique, the corresponding prediction rate curve in Fig. 7 can provide a measure of space-robustness.

7. Conclusions

In this study, a case study for landslide stability analysis under GIS environment and landslide prediction modeling was carried out using data sets of Boeun area, Korea. After extraction of hydrological factors and topographically based indices of hydrological landslide characteristics, stability index mapping approach and the followed S-A plot were also performed with landslide point features. As a result, major characteristics are revealed, but high possibility of hidden landslide occurrences or potential initiation zones is also expected. As for S-A plot, if actual measurements are applied, this plot is regarded as an important result to characterize landslide areas, because it contains

hydrological information such as stability index with actual occurrences and wetness index, according to contributing catchment area and soil friction angle.

For landslide prediction modeling, we exemplified how data mining can be used to assess the degree of support provided by the spatial data that were used to represent the physical conditions in the neighborhoods of the known landslides and to extrapolate them to those of other unknown future landslides. Owing to the spatial partitioning of the landslide distribution, the validation strategy provides some empirical measures of support in the prediction of “where the landslides are likely to occur”. We must stress that significance of the prediction is only within the validation results or degree of satisfaction for the spatial matching of hazard ranges and the relative distribution of validation landslides. This validation result and its interpretation are useful as pieces of “heuristic supporting information”, not only for evaluating the space-robustness of the prediction models, but also for analyzing the landslides that had occurred at the neighboring areas.

In this paper, these two tasks were independently processed for preparation of unbiased criteria, and then results of those were qualitatively compared. As results, land stability analysis based on DEM-based hydrological variables directly reflects terrain characteristics; however, results in the form of land stability map by landslide prediction model is not fully matched due to heuristic scheme within prediction approach. Therefore, it is expected that the results on the space-robustness of landslide prediction models in conjunction with DEM-based landslide stability analysis can be effectively utilized to search out unrevealed or hidden landslide occurrences. Also, this kind of approach will be further utilized to delineate hydrological characteristics of large-scale watersheds, even to small-scale ones, related to landslide occurrence.

For the future works related to prediction modeling, some aspects will be considered. The important tasks in

spatial prediction model are that one is the choice of prediction model and the other is the selection of relevant data layers which contain useful information in causal factors. We are currently analyzing the selection of causal factors, and evaluating other prediction models such as fuzzy logic model and evidential reasoning approach.

References

- An, P., W. M. Moon, and A. Rencz, 1991. Application of fuzzy set theory to integrated mineral exploration, *Canadian Journal of Exploration Geophysics*, 27(1): 1-11.
- Chi, K. H., Shin, J. S., and Park, N.W. 2001. Quantitative analysis of GIS-based landslide prediction models using prediction rate curve, *Korean Journal of Remote Sensing*, 17(3): 199-210.
- Chung, C. F., and A. G. Fabbri, 1993. The representation of geoscience information for data integration, *Nonrenewable Resources*, 2(2): 122-139.
- Chung, C.F., and A.G. Fabbri, 1998. Three Bayesian prediction models for landslide hazard. In, Bucciannti, ed., *Proceedings of International Association for Mathematical Geology Annual Meeting (IAMG'98)*, Ischia, Italy, October 3-7, 1998: 204-211.
- Chung, C. F., and A. G. Fabbri, 1999. Probabilistic prediction models for landslide hazard mapping, *Photogrammetric Engineering & Remote Sensing*, 65(12): 1389-1399.
- Chung, C.F., H. Kojima, and A.G. Fabbri., 2001. Stability analysis of prediction models for landslide hazard mapping, In, R.J. Allison, ed., *Applied Geomorphology: theory and practice*, John Wiley & Sons, Ltd (in press).
- Davis, K. M., 2000. *Object-oriented Modeling of Rivers and Watersheds in Geographic Information Systems*, M.Sc. Thesis (Unpublished), The University of Texas at Austin: 133.
- Dietrich, W. E., C. J. Wilson, D. R. Montgomery and K. McKean. 1993. Analysis of erosion thresholds, channel networks, and landscape morphology using a digital terrain model, *Journal of Geology*, 101: 259-278.
- Fabbri, A.G., and C.F. Chung, 2001. Spatial support in landslide hazard predictions based on map overlays, *Proceedings of International Association for Mathematical Geology Annual Meeting (IAMG 2001)*, Cancun, Mexico, September 10-12, 2001., CDROM.
- Garbrecht, J. and L. W. Martz, 1997. The Assignment of Drainage Direction over Flat Surfaces in Raster Digital Elevation Models, *Jour. of Hydrology*, 193: 204-213.
- Hellweger, F. L. and D. R. Maidment, 1999. Definition and Connection of Hydrologic Elements using Geographic Data, *Journal of Hydraulic Engineering*, 4: 10-18.
- Mason, D. and D. R. Maidment, 2000. An Analysis of a Methodology for Generating Watershed Parameters using GIS, *CRWR Online Report 00-3*: 202.
- Montgomery, D. R. and W. E. Dietrich, 1994. A physically based model for the topographic control on shallow landsliding, *Water Resources Research*, 30(4): 1153-1171.
- Montgomery, D. R., K. Sullivan, and H. W. Greenberg, 1998. Regional test of a model for shallow landsliding, *Hydrological Processes*, 12: 943-955.
- Moon, W. M., 1990. Integration of geophysical and geological data using evidential belief function, *IEEE Trans. Geoscience and Remote Sensing*, 28(4): 711-720.
- O'Loughlin, E. M., 1986. Prediction of surface saturation zones in natural catchments by topographic

- analysis, *Water Resources Research*, 22(5): 794-804.
- Pack, R. T., D. G. Tarboton, and C. N. Goodwin, 1998. Terrain stability mapping with SINMAP. Technical description and users guide for version 1.00, *Terratech Consulting Ltd., Report No. 4114-0*, Salmon Arm, B.C., Canada, p 68.
- Smith, T. R., B. Birnir and G. E. Merchant, 1997. Towards an Elementary Theory of Drainage Basin Evolution: The Theoretical Basis, *Computers and Geosciences*, 23(8): 811-822.
- Tarboton, D. G., 1997. A New Method for the Determination of Flow Directions and Contributing Areas in Grid Digital Elevation Models, *Water Resources Research*, 33(2): 309-319.
- Wilson, J. P., H. Mitasova, and D. J. Wright, 2000. Water Resources Applications of Geographic Information Systems, *URISA Journal*, 12(2): 61-79.
- Wu, W. and R. C. Sidle, 1995. A distributed slope stability model for steep forested basins, *Water Resources Research*, 31(8): 2097-2110.
- Van Westen, C.J., 1993. *Application of geographic information systems to landslide hazard zonation*, Ph.D. Thesis, Technical university of Delft, International Institute for Aerospace Survey and Earth Sciences, The Netherlands, ITC publication 15(1): 245.